A Phase Velocity Filter for the Measurement of Lamb Wave Dispersion

Chris Adams, Sevan Harput, David Cowell and Steven Freear
Ultrasonics and Instrumentation Group,
School of Electronic and Electrical Engineering,
University of Leeds, Leeds,
LS2 9JT, UK
Email: elca@leeds.ac.uk

***Abstract*—The complex, multi-modal and dispersive nature of guided waves makes them extremely effective in the non destructive evaluation of plate-like structures. Knowledge of the dispersion relation of a material is a prerequisite to many guided wave experiments. A frequency-phase velocity map is by far the most useful representation of dispersion. These phase velocity curves can be obtained numerically by solving the Lamb equations, however instabilities and unfamiliarity with the specimen's parameters makes experimentally obtained dispersion relation desirable. Transformations can be applied to an experimentally obtained frequency-wave number map but it requires prohibitively high number of sampling points in space to resolve modes across the full bandwidth of the transducer. The phase velocity filter described here is able to extract wavelets of a particular phase velocity irrespective of frequency. When applied to the acquisition of dispersion relation, the technique exhibits reduced artefacts and is able to extract modes across the full bandwidth of the excitation. Results show a bandwidth increase of approximately 58%.**

I. Introduction

Guided waves which consist of multiple modes of oscillation, are inherently complex, but are now well understood. At any given frequency, an infinite number of modes exist [1]. They can be either symmetric or antisymmetric in shape.

Each mode has a unique dispersive relationship between frequency, group velocity (C_g), phase velocity (C_{ph}), and attenuation [2]. Some authors have presented techniques for compensating for the dispersion [3]. This relationship and physical structure makes their interaction with defects unique [1]. Higher order modes can couple into corrosion and can be used for the evaluation of texture versus low order modes which are useful in the evaluation of larger defects. Recently, lamb waves have been applied to the measurement of bone thickness [4].

The measured frequency-phase velocity representation of this dispersion is useful as high order modes are particularly prone to velocity changes [5] and measured velocity can also indicate the thickness of a material [6]. It is also the most useful representation in experimental design [7]: the phase velocity can be directly obtained for time of flight experiments [8] as can its corresponding wavelength (λ) using $C_{ph} = f\lambda$. This property is critical in many experiments where mode control is required.

These dispersion curves can be generated by solving the Lamb equations. All the parameters for calculation may not be available to the engineer, and solutions become more complex when composite materials are used. Additionally, numerical instabilities around high frequency-thicknesses (fd) make experimental validation of dispersion curves highly desirable.

In anisotropic solids, a π shift [10] or zero crossing [11] in time can be introduced through displacement for the measurement of phase velocity . This is difficult to achieve reliably at high frequencies [10] and is particularly inappropriate for lamb waves as they are multi-modal. The amplitude spectrum method is more appropriate for solids with close proximity boundaries but is still not applicable to multi modal waves [12]. When dealing with only low order modes, a wavelet transform can be used to separate modes [13]. Singular value decomposition can also be utilised but gives coarse results with better contrast however [7]. When possible, laser vibrometetry can be used in conjunction with Snell's law to generate dispersion plots [14]. This however is time consuming. For measurement of group velocity, from which phase velocity can be derived [9], spectral decomposition can be used [15].

Experimentally, the two dimensional Fourier transform is most commonly used for the separation of modes from time domain signals [16], [17]. Fourier analysis can also be performed on smaller segments of the recorded signals to produce time-frequency maps [18]. By measuring the surface displacement at many points along the surface of a wave guide, a matrix of time-space dimensionality can be obtained. When the Fourier transform is applied a wavenumber-frequency map can be obtained. Since $k = 1/\lambda = f/C_{ph}$, elements can be re-arranged to form a phase velocity dispersion map [7], [19]. This works well, but requires prohibitively high sampling frequencies and spatial measurement intervals to produce convincing results.

Here, a phase velocity filter is presented as a solution to this problem. The filter is able to extract waves of particular phase velocities irrespective of the frequency content. Using less measurement points with experimentally feasible time and space sampling intervals, phase velocity maps with improved definition and reduced error can be produced.

II. METHOD

In this section the concept behind the phase velocity filter is given. This can be implemented digitally, and will be described in the section following. This filter is used for the generation of a phase velocity dispersion map. Simulation parameters for the generation of such an map will be given.

A. Concept

When the temporal frequency of guided waves are known, delays can be applied to each element when an array is in receive of guided waves to temporally align particular modes, such that when they are summed, constructive interference takes place. Thus, when the engineer has knowledge of a specimen's dispersion curve and excitation frequency, delays can be chosen as to assess the existence of a particular mode [20]. This relationship is described in Equation 1.

$$\lambda = \frac{L}{\beta + (t_0/T)} \tag{1}$$

Here, λ is wavelength, L is pitch, β is an arbitrary integer and t_0 is the delay increment to be applied to each element. T is simply $1/f$.

Substituting $C_{ph} = f\lambda$ and $T = 1/f$ means the time delay can be expressed as a function of phase velocity and frequency, as in Equation 2.

$$t_0 = \frac{L}{C_{ph}} - \frac{1}{f} \tag{2}$$

Since any time domain signal can be expressed as an infinite sum of its constituent frequency components, frequency dependent delays can be applied to the incoming signals to filter a phase velocity irrespective of its frequency.

B. Digital Implementation

Consider $x(n,m)$, a time domain signal of N samples recorded at interval n from element m of an array transducer. Its discrete Fourier transform (in time only) is $X(k,m)$, which is described in Equation 3 and defined in 4.

$$x(n,m) \xrightarrow{\mathscr{F}} X(k,m) \tag{3}$$

$$X(k,m) = \sum_{n=0}^{N-1} x(n,m) e^{\frac{-j2\pi nk}{N}} = A_k e^{j\phi_k} \tag{4}$$

These complex coefficients represent the amplitude and phase of an exponential function. When these weighted exponential functions are summed, the original time domain signal can be obtained. A time delay in the time domain maps to a phase delay in the frequency domain. Equation 5 describes this relationship when a delay of D samples is applied to the original time domain signal.

$$x(n-D,m) \xrightarrow{\mathscr{F}} e^{\frac{-j2\pi kD}{N}} X(k,m) \tag{5}$$

D can be replaced by $D(k,m,C_{ph})$, a function of frequency, element position and phase velocity. Firstly the substitution

$$f = k \times \frac{f_s}{2N}$$

is applied to Equation 1 yielding Equation 6.

$$\frac{L}{C_{ph}} - \frac{2N}{kf_s} \tag{6}$$

Here, f_s is the sampling frequency and the assumption is made that when $k = N$, $f = fs/2$, the Nyquist limit. Since Equation 6 describes the real time delay applied in seconds per element, $D(k,m,C_{ph})$ can be derived by multiplying each instance of m by mf_s to obtain a value in samples for each element:

$$D(k,m,C_{ph}) = \begin{cases} m \times \frac{Lf_s}{C_{ph}} - \frac{2N}{k}, & \text{for } k > 0, \\ 0, & \text{for } k = 0 \end{cases} \tag{7}$$

When $k = 0$ (DC), $D = -\infty$, so conditions are applied to prevent this. This is not problematic, since phase velocity is zero at DC.

This forms the basis of the digital implementation of the phase velocity filter. When D in Equation 5 is replaced with $D(k,m,C_{ph})$. It's possible to temporally align all frequency components across the transducer array.

C. Application: Phase Velocity Image Generation

The derivation of Equation 7 makes it possible to temporally align all frequency components across the array for a given phase velocity. There are many potential applications of this. Here, it will be explained how frequency-velocity dispersion maps can be obtained using the filter.

Consider the two dimensional matrix, $x(n,m)$ again. In Equation 8, following Fourier analysis in the time dimension, a new three dimensional matrix, Y is created by evaluating for a number of discrete values of C_{ph}. The interval, number and range is the choice of the designer. As before, the n dimension represents N points in time and m represents M elements in space. In essence, time-amplitude signals for each element m are concatenated together to form the matrix.

$$Y(k,m,o) = X(k,m) \times e^{\frac{-j2\pi kD(k,m,C_{ph})}{N}} \forall o \in C_{ph} \tag{8}$$

Applying the inverse Fourier transform and summing in dimension m yields the matrix y in Equation 9. This is divided by M to conserve energy, although is not strictly required.

$$y(n,o) = \frac{\sum_{m=0}^{M-1} \mathscr{F}^{-1}\{Y(k,m,o)\}}{M} \tag{9}$$

y is a series of time domain signals for each evaluated phase velocity, o. Constructive interference will have taken place at particular frequencies and phase velocities. Finally, the frequency-velocity matrix S is found by applying the Fourier transform as in Equation 10.

$$S(k,o) = \mathscr{F}\{y(n,o)\} \tag{10}$$

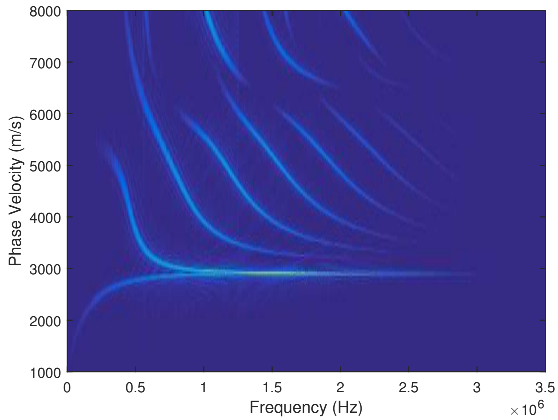

Fig. 1. High resolution frequency-phase velocity map produced using re-ordering of the frequency-wave number matrix. The map exhibits excellent resolution and definition but is computationally expensive and difficult to achieve experimentally

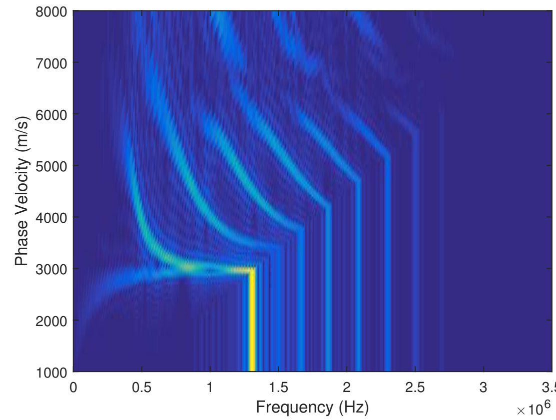

Fig. 2. Low resolution frequency-phase velocity map produced using re-ordering of the frequency-wave number matrix. Before being processed, the space-time matrix has been decimated to better represent the spatial properties of a transducer. All lamb modes and S waves are visible, but there is some loss of information and an increase in artefacts

D. Simulation Parameters

The technique is demonstrated in simulation using an FEA tool. The specimen is a 5 mm thick Aluminium sheet. At one end a Blackman-Harris shaped pulse pressure load is applied with a centre frequency of 1.5 MHz. Matrix x is created from the shear displacement at each node on the surface.

For comparison, a phase velocity map at full resolution will be generated using the $C_{ph} = f/k$ transformation applied to the two dimensional Fourier transform of x which gives a frequency-wave number map. Then the matrix is decimated so each waveform is spatially separated by 1 mm, and the number of elements is reduced to 64; this is to better emulate the physical properties of an array probe. A velocity map will again be produced using substitution on the decimated matrix. Finally, the new filter will be used to generate a map.

In every case 256 values of C_{ph} are tested between 1000 and 8000 m/s. The sampling frequency is 101 MHz.

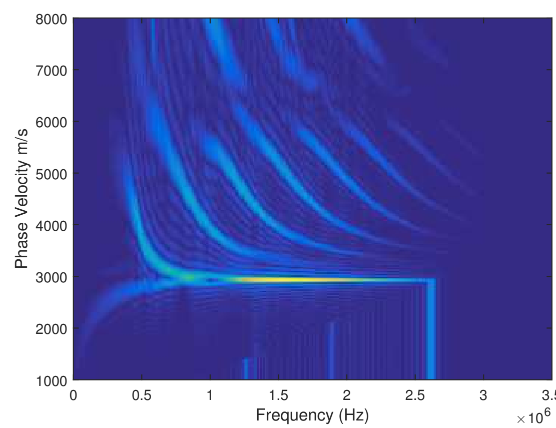

Fig. 3. A frequency-phase velocity map produced by iteratively filtering phase velocities. All lamb waves and S waves are visible. Artefacts are introduced at low phase velocities but they do not impinge on the modes

III. Results and Discussion

Figure 1 shows a phase velocity map generated with a high resolution matrix taken from every available node in the simulation. For each value of C_{ph} and f, the corresponding element in the frequency-wave number domain is found using the relationship $C_{ph} = f/k$. All Lamb modes and S waves, are visible and well defined; the lines appear thin and are well contrasted against the noise floor. They are of equal magnitude, although as expected, there is some loss of energy as the fringes of the Blackman-Harris window are reached. The results align extremely well with theoretical results. The map exhibits excellent resolution in both dimensions.

Figure 2 shows the same technique applied to a reduced matrix. Here, the time space matrix has been reduced so that only 64 elements are used, they are spaced by 1 mm. This emulates a typical NDE transducer's spatial properties. The map is not as well defined as in Figure 1. The smaller wave number dimension means that there is a loss of phase velocity information, as such, the modes cannot be resolved across their whole frequency range. This introduces artefacts into the map which begin to dominate as the frequency increases. In every case there is blurring and quantisation errors at higher phase velocities. A lower contrast contributes to the poor definition of each mode and ghosting is visible.

Finally, in Figure 3 a frequency-phase velocity map generated by iteratively performing phase velocity filtering and then applying a Fourier transform on the decimated array is presented. The Lamb and S-wave modes can be resolved across the whole frequency range. Zero padding before filtering has resulted in the introduction of some artefacts at low phase velocities, this is not problematic however as they do not interfere with the modes.

Figure 1, which uses matrix re-ordering is the best of the three results presented. This technique is computationally inefficient; the wave number matrix used here is obtained from 5077 positions. This number of measurements is not feasible experimentally as even the most dense of transducer array probes are typically limited to 256 elements. When the matrix is decimated to use a realistic element separation and only 16 elements it becomes apparent that this technique is not appropriate for use experimentally. With the reduced matrix, noise, artefacts and quantisation errors mean that the modes cannot be resolved across their full frequency range. Conversely, the proposed technique is able to resolve the modes across more of the frequency range.

IV. Conclusion

Guided waves are complex in nature and consist of many antisymmetric and symmetric modes. Each mode's phase velocity has a unique relationship with frequency. This complex nature can be leveraged in a variety of NDE problems. Visualising the phase velocity is often the most useful in experiment design as the wavelength can be easily ascertained as can the velocity. Phase velocity of modes can be calculated by numerically solving lamb equations, however, instability at high frequency-thicknesses and unfamiliarity with a material's parameters makes experimental validation expedient.

Experimentally, the frequency-wave number representation is used to separate modes from spatially separated time domain signals. However, in this domain it is harder to distinguish each mode. The matrix can be shuffled into a phase velocity map but this requires a high number of spatial sampling points to produce effective results and even if experimentally feasible, it is computationally expensive.

It is shown that phase velocity filtering could be achieved with an array probe, from which a space-time matrix can be formed. A two dimensional filter can be designed in the space-frequency domain to align wave packets of the supplied phase velocity irrespective of their frequency. After this filter is applied the matrix can be summed in the time domain to find the constructively interfering (across space) content.

Time domain signals filtered for a number of phase velocities are obtained, these are then transformed into the frequency domain to produce frequency dependent phase velocity maps. These maps are not free from artefacts and noise, but are superior in experimental circumstances to array re-ordering. It is shown that in situations where only a modest or even plentiful arrays are used, artefacts hinder full frequency resolution of the modes when using re-ordering.

This research has shown that it is possible to filter an arbitrary phase velocity in a guided wave experiment. The applications of this are diverse, but as an example, it has been applied to the generation of phase velocity dispersion relation map. These maps are usually generated by re-ordering a frequency-wave number matrix. It is shown that when using the phase velocity filter to generate the map, superior results can be obtained.

The generation of a phase velocity dispersion map is just one potential application of the phase velocity filter, and serves well as a proof of concept. However, further research might involve its application to NDE problems where the velocity is directly used as a quantifier. The measurement of corrosion depth is an example.

References

[1] D. N. Alleyne and P. Cawley, "Optimization of lamb wave inspection techniques," *Ndt & E International*, vol. 25, no. 1, pp. 11–22, 1992.

[2] M. ODonnell, E. Jaynes, and J. Miller, "Kramers–kronig relationship between ultrasonic attenuation and phase velocity," *The Journal of the Acoustical Society of America*, vol. 69, no. 3, pp. 696–701, 1981.

[3] S. Fu, L. Shi, Y. Zhou, and J. Cai, "Dispersion compensation in lamb wave defect detection with step-pulse excitation and warped frequency transform," *IEEE Transactions on Ultrasonics, Ferroelectrics, and Frequency Control*, vol. 61, no. 12, pp. 2075–2088, Dec 2014.

[4] J. Foiret, J. G. Minonzio, C. Chappard, M. Talmant, and P. Laugier, "Combined estimation of thickness and velocities using ultrasound guided waves: a pioneering study on in vitro cortical bone samples," *IEEE Transactions on Ultrasonics, Ferroelectrics, and Frequency Control*, vol. 61, no. 9, pp. 1478–1488, Sept 2014.

[5] W. Lin, X. Li, and J. q. Wang, "Study on relationship between the lamb wave velocity and fatigue of plate," in *Piezoelectricity, Acoustic Waves and Device Applications (SPAWDA), 2011 Symposium on*, Dec 2011, pp. 260–263.

[6] E. Moreno and P. Acevedo, "Thickness measurement in composite materials using lamb waves," *Ultrasonics*, vol. 35, no. 8, pp. 581–586, 1998.

[7] J.-G. Minonzio, M. Talmant, and P. Laugier, "Measurement of guided mode wave vectors by analysis of the transfer matrix obtained with multi-emitters and multi-receivers in contact," in *Journal of Physics: Conference Series*, vol. 269, no. 1. IOP Publishing, 2011, p. 012003.

[8] L. Mažeika, L. Draudvilienė, and E. Žukauskas, "Influence of the dispersion on measurement of phase and group velocities of lamb waves," *Ultrasound*, vol. 64, no. 4, pp. 18–21, 2009.

[9] W. Simpson and D. McGuire, "Phase and group velocities for lamb waves in dop-26 iridium alloy sheet," Oak Ridge National Lab., TN (United States), Tech. Rep., 1994.

[10] W. Sachse and Y.-H. Pao, "On the determination of phase and group velocities of dispersive waves in solids," *Journal of Applied Physics*, vol. 49, no. 8, pp. 4320–4327, 1978.

[11] L. Mažeika and L. Draudvilienė, "Analysis of the zero-crossing technique in relation to measurements of phase velocities of the lamb waves," *Ultrasound*, vol. 66, no. 2, pp. 7–12, 2010.

[12] T. Pialucha, C. Guyott, and P. Cawley, "Amplitude spectrum method for the measurement of phase velocity," *Ultrasonics*, vol. 27, no. 5, pp. 270–279, 1989.

[13] D. Waltisberg and R. Raišutis, "Group velocity estimation of lamb waves based on the wavelet transform," *Ultragarsas (Ultrasound)*, vol. 63, no. 4, pp. 35–40, 2008.

[14] M. Harb and F. Yuan, "Non-contact ultrasonic technique for lamb wave characterization in composite plates," *Ultrasonics*, vol. 64, pp. 162 – 169, 2016.

[15] L. Draudvilienė and L. Mažeika, "Measurement of the group velocity of lamb waves in aluminium plate using spectrum decomposition technique," *Ultragarsas" Ultrasound"*, vol. 66, no. 4, pp. 34–38, 2012.

[16] D. Alleyne and P. Cawley, "A two-dimensional fourier transform method for the measurement of propagating multimode signals," *The Journal of the Acoustical Society of America*, vol. 89, no. 3, pp. 1159–1168, 1991.

[17] D. N. Alleyne and P. Cawley, "A 2-dimensional fourier transform method for the quantitative measurement of lamb modes," in *Ultrasonics Symposium, 1990. Proceedings., IEEE 1990*. IEEE, 1990, pp. 1143–1146.

[18] M. Niethammer, L. J. Jacobs, J. Qu, and J. Jarzynski, "Time-frequency representations of lamb waves," *The Journal of the Acoustical Society of America*, vol. 109, no. 5, pp. 1841–1847, 2001.

[19] B. Ren and C. J. Lissenden, "Pvdf multielement lamb wave sensor for structural health monitoring," *IEEE transactions on ultrasonics, ferroelectrics, and frequency control*, vol. 63, no. 1, pp. 178–185, 2016.

[20] J. Li and J. L. Rose, "Implementing guided wave mode control by use of a phased transducer array," *IEEE transactions on ultrasonics, ferroelectrics, and frequency control*, vol. 48, no. 3, pp. 761–768, 2001.